J. Membrane Biol. 3, 123 – 141 (1970)
© by Springer-Verlag New York Inc. 1970

Water Permeability of Phospholipid Vesicles

J. P. REEVES* and R. M. DOWBEN**

Department of Biology, Massachusetts Institute of Technology, Cambridge, Massachusetts 02139

Received 24 March 1970

Summary. The water permeability of phospholipid vesicles 0.5 to 10 μ in diameter bounded by one or by several lipid bilayers was measured by following the change in turbidity of a suspension after mixing in a stopped flow apparatus. A semi-empirical formulation for evaluating volume changes of vesicles with a broad size range by measurement of turbidity is developed. The rate of flow is analyzed in terms of reaction rate theory. The water permeability coefficients for phosphatidylcholine vesicles were approximately 44 μ/sec at 25 °C and 70 μ/sec at 37 °C. The activation energy for water transport was 8.25 kcal/mole. The results were consistent with the view that water permeates by dissolution and diffusion in the membrane.

In recent years, efforts have been made to develop and utilize phospholipid model systems for investigating membrane phenomena with the view that such studies might help elucidate processes which occur in natural membranes. One model system that has been used widely involves the formation of a bimolecular lipid leaflet 1 to 2 mm in diameter in the aperture of a plastic diaphragm separating two aqueous solutions (Mueller, Rudin, Tien & Wescott, 1963; Huang, Wheeldon & Thompson, 1964). Another model system consists of fragmented myelin figures formed by agitating a suspension of hydrated phospholipids (Rendi, 1964; Bangham, Standish & Watkins, 1965). In a previous communication (Reeves & Dowben, 1969), we described the preparation and some properties of phospholipid vesicles 0.5 to 10 μ in diameter bounded by one (or a few) phospholipid bilayers.

As a model system, the phospholipid vesicles possess a number of virtues. Vesicles can be prepared in large quantities from pure phospholipids or from a phospholipid mixture of known composition. After an experiment,

* Present address: Department of Microbiology, Rutgers University, New Brunswick, N.J. 08903.

** Present address: Division of Biological and Medical Sciences, Brown University, Providence, R.I. 02912.

the vesicles can be harvested and their composition determined, for example, by thin layer chromatography. Because they are mechanically stable, withstanding pipetting and centrifugation, and because suspensions possess large total surface areas, vesicle preparations lend themselves to permeability studies.

In this communication, studies of the water permeability of such phospholipid vesicles are reported. Volume changes of the vesicles in a suspension were assessed from turbidity measurements. Owing to the range of vesicle diameters, and to the tendency of the small vesicles (with a high surface/volume ratio) to reach equilibrium more rapidly, the turbidity changes after suddenly shifting the osmolarity of the suspending medium are complex. Expressions were developed for turbidity changes taking into account a vesicle population with a range of diameters, as well as expressions for water flow in terms of rate theory.

Materials and Methods

Preparation and Storage of Phosphatidylcholine

Pure phosphatidylcholine was isolated from a chloroform extract of egg yolks by chromatography on alumina and silicic acid columns (Ansell & Hawthorne, 1964). The product migrated as a single spot when analyzed by thin layer chromatography with 80:25:3 chloroform-methanol-water used as developer. The lipid was stored under nitrogen as a 10^{-2} M solution in benzene (thiophene-free, reagent grade). For long-term storage, the benzene solution was sealed in ampoules under nitrogen, and stored in the dark at -30 °C. Lipid oxidation was assessed by the thiobarbituric acid (TBA) test (Ottolenghi, 1959). The lipids appeared to oxidize gradually after preparation, even when stored in sealed ampoules in a deep freeze.

Vesicle Formation

Phosphatidylcholine vesicles were prepared in 0.2 M sucrose as described previously (Reeves & Dowben, 1969). The swelling medium was degassed using a water aspirator in an effort to minimize lipid oxidation. To avoid exposing the dried lipids to air, the swelling flask was equipped with a separatory funnel through which the medium was added. Swelling was carried out at 42 °C. No fresh phospholipid preparations would form vesicles at room temperature; only highly oxidized lipids (TBA test OD > 0.2 for a sample containing 2 μmoles phospholipid) formed vesicles at room temperature.

Turbidity Measurements

Turbidity measurements were made in a Zeiss PMQ II spectrophotometer using quartz semimicro cells. The entrance portal to the sample chamber was equipped with a series of diaphragms so that the entrance slit could be adjusted. Smaller slit widths tended to reduce the amount of scattered light falling on the photomultiplier; thus, higher ex-

tinctions generally were obtained with smaller slit widths. For most measurements, the smallest slit width (<1.0 mm) was used.

Vesicles suspended in 0.2 M glycine were mixed rapidly with an equal volume of 0.6 M glycine and the optical density (OD) observed as a function of time using a stopped flow apparatus (French, Benkovic & Bruice, 1965) fitted into the sample chamber of the spectrophotometer. The half time of the OD change provided a measure of the permeability coefficient (*see* below). The temperature of the apparatus was maintained within ± 0.1 °C in a Haake type F circulating water bath. The output of the Zeiss spectrophotometer was amplified and fed into a Brush oscillograph (model 16-2300). The amplifier was constructed from an RCA integrated circuit (CA 3005) in the differential amplifier configuration. Emitter followers were used to match the impedances of the oscillograph and the amplifier.

When distilled water and 0.6 M glycine or a vesicle suspension and isosmotic glycine were mixed in the stopped flow apparatus, the OD stabilized within 0.1 sec. For all measurements, zero time was assumed to be 0.1 sec after the plunger was stopped. All solutions used in the stopped flow apparatus were degassed with a water aspirator to prevent cavitation.

For one series of measurements (preparation C in Table 2 and Fig. 7), a mercury lamp was used for the light source and an RCA IP 28 photomultiplier served as the detector. An interference filter with maximum transmittance at 546 nm was inserted between the light source and the stopped flow apparatus. The output of the photomultiplier was amplified by a differential amplifier constructed from an RCA 3001 integrated circuit and fed into the oscillograph.

When the stopped flow apparatus was used in conjunction with the Zeiss spectrophotometer, the extinction of the vesicles was nearly the same as in measurements carried out in the semimicro cells. The extinction was much lower in the mercury lamp-photomultiplier system. However, the kinetics of the OD changes observed in the permeability experiments were identical in the two systems.

Optical Properties of the Vesicles

The turbidity of a dilute suspension of colloidal particles (Hochgesang, 1964) obeys the relation

$$\mathrm{OD} = \log I_0/I = 0.434\,\varepsilon\, b\, N \tag{1}$$

where OD is the optical density, I_0 and I the intensities of the incident and transmitted light, respectively, ε the extinction coefficient, b the path length of light travelling through the suspension, and N the number of particles per cc. For a suspension of homogeneous spheres, large compared to the wavelength of the incident light, with a refractive index near that of the surrounding medium, the extinction coefficient is given by (van de Hulst, 1957; Koch, 1961)

$$\varepsilon = \pi a^2 \left[2 - \frac{4}{\rho}\sin\rho + \frac{4}{\rho^2}(1-\cos\rho)\right] \tag{2}$$

where $\rho = 4\pi a(m-1)/\lambda$, a is the radius of the sphere, λ the wavelength of incident light in the external medium, and m the ratio of refractive index of the sphere to refractive index of the medium. Expressing $\sin\rho$ and $\cos\rho$ as a power series, Eq. (2) becomes

$$\varepsilon = \frac{\pi a^2 \rho^2}{2}\left[1 - \frac{\rho^2}{18} + \frac{\rho^4}{720} - \cdots\right]. \tag{3}$$

For small values of ρ, Eq. (3) reduces to[1]

$$\varepsilon = \frac{\pi a^2 \rho^2}{2} = \frac{8\pi^3 a^4}{\lambda_0^2}(n_s - n_m)^2 \tag{4}$$

where n_s and n_m are the refractive indices of the spheres and the surrounding medium respectively, and $\lambda_0 = n_m \lambda$ is the wavelength of the incident light.

For a suspension of spheres with a range of diameters, a^4 is replaced by $\langle a^4 \rangle$, the average value of the radius to the fourth power, which is defined by

$$\langle a^4 \rangle = \int_0^\infty a^4 P(a)\, da \tag{5}$$

where $P(a)$ is the probability density function for the distribution of vesicle radii.

Eqs. (1), (4) and (5) will be taken as an approximate description of the light-scattering properties of a suspension of phospholipid vesicles. The effect of scattering by the vesicle walls has been neglected. In addition, it should be noted that Eq. (4) is strictly valid only when the particles are large compared to the wavelength of light. Although the particles in these experiments are comparable in size to the light wavelength, Eq. (4) provides a good approximation of more rigorous and complex formulations (Koch, 1961). It will be shown below that these equations predict approximately some measured turbidity properties of vesicle suspensions.

Figs. 1–3 show that the turbidity of a vesicle suspension is a linear function of N, $(n_s - n_m)^2$, and λ^{-2} as expected from the above relations. The slight curvature of the data in Fig. 1 is very likely due to multiple scattering. The lines in Figs. 2 and 3 do not pass through the origin as predicted by theory; the positive intercept at zero refractive index difference in Fig. 2 probably represents scattering by the membrane walls of the vesicles.

The slopes of the experimental curves are compared with those predicted from theory in Table 1. Because the vesicle diameters follow a log normal distribution (Reeves &

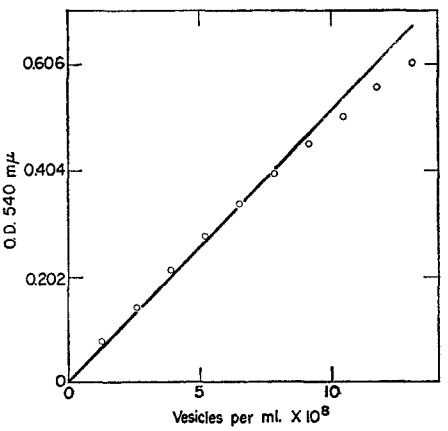

Fig. 1. Optical density of vesicles plotted against concentration. Vesicles were prepared in 0.2 M sucrose and suspended in 0.2 M glycine. The vesicle count of the suspension was determined with a Petroff-Hauser counting chamber. Samples of the suspension were diluted to give the concentrations shown in the figure

1 In these experiments, $(m-1)$ is about 5×10^{-3}, $\lambda = 0.405$ μ, a varies from 0.5 to 8 μ and ρ varies from about 0.078 to 1.24. Even for the higher values of ρ, the error arising from neglecting the higher terms of Eq. (3) is very small.

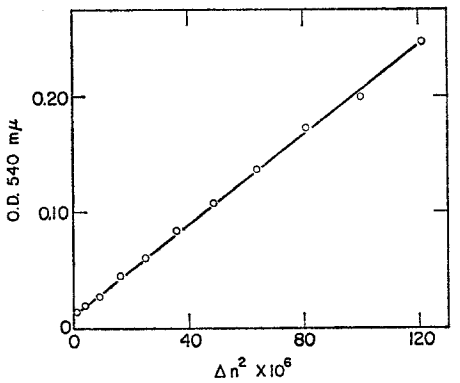

Fig. 2. Optical density of vesicles *vs.* the square of the refractive index difference (Δn^2). Vesicles were prepared in 0.4 M sucrose and suspended in 0.4 M (0.385 osmolar) glycine. Samples of the suspension were placed in isosmolar mixtures of sucrose and glycine. The refractive index of the medium was varied by adjusting the proportions of sucrose and glycine. The internal refractive index was assumed to be the refractive index of 0.385 osmolar sucrose (1.3500). The refractive index of the medium was calculated from the measured refractive indices of the original sucrose and glycine media and their proportions in the medium. Refractive indices were measured using a Bausch and Lomb hand refractometer

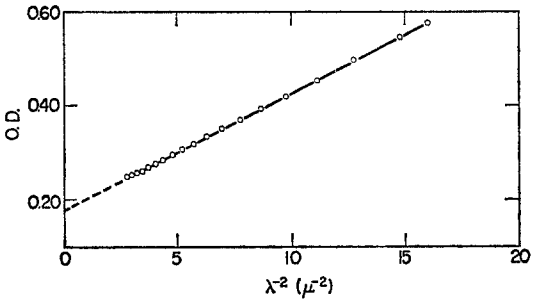

Fig. 3. Spectrum of a suspension of vesicles. Vesicles were prepared in 0.4 M sucrose and suspended in 0.4 M glycine. The OD of the suspension was determined at 20-nm intervals in the range 250 to 600 nm

Table 1. *Agreement of measured OD with predictions from theory*

Abscissa	N	Δn^2	Theoretical slope OD[a]	Experimental slope OD[b]
Δn^2	1.5×10^8	—	3.81×10^3	2.06×10^3
λ^{-2}	2.4×10^8	1.17×10^{-4}	2.08×10^{-9}	0.25×10^{-9}
N	—	3.6×10^{-5}	9.15×10^{-10}	5.18×10^{-10}

[a] Calculated from Eqs. (3) and (4) using the data given above.
[b] Obtained directly from Figs. 1 – 3.

Dowben, 1969), the value for the average particle radius can be calculated directly from

$$P(a)\,da=\frac{1}{\sqrt{2\pi}\log\sigma_s}\exp\left[-\frac{(\log a-\log a_g)^2}{2\log^2\sigma_g}\right]d(\log a) \tag{6}$$

where a_g is the geometric mean diameter, and σ_g the geometric standard deviation Substituting Eq. (6) into Eq. (5) and integrating yields

$$\log\langle a^4\rangle=4\log a_g+18.42\log^2\sigma_g. \tag{7}$$

The values $a_g=0.87$ μ and $\sigma_g=1.74$ μ were obtained by measuring several hundred phosphatidylcholine vesicles in phase-contrast micrographs; substituting these values into Eq. (7) gives $\langle a^4\rangle=(1.62\ \mu)^4$.

The observed slopes for plots of OD *vs.* Δn^2 and N are about 55% of the theoretical slopes; for OD *vs.* λ^{-2}, the experimental slope is only 12% of the theoretical value. These discrepancies probably result from the unfavorable geometry of the spectrophotometer Particles the size of vesicles scatter radiation predominantly in a small solid angle about the transmitted beam (Billmeyer, 1964). Unless the receptive cone of the light detector of the spectrophotometer is extremely small, a substantial portion of this scattered radiation falls on the phototube, thus lowering the turbidity. The fraction of scattered radiation reaching the detector, and thus the error in the measured extinction coefficient, increases with increasing particle size and decreasing wavelength.

Calculation of Turbidity Changes

The OD of vesicles suspended in hypertonic[2] media will increase with the osmolarity of the medium. The ratio of the OD of vesicles suspended in a hypertonic medium to the OD of vesicles in an isotonic medium can be derived from Eqs. (1), (4) and (5) as

$$\frac{\mathrm{OD}}{\mathrm{OD}_0}=\frac{a^4(n_s-n_m)^2}{a_0^4(n_{s,0}-n_m)^2} \tag{8}$$

where the zero subscripts refer to isotonic conditions. The refractive index of the vesicle can be expressed as

$$n_s=n_w+\alpha'\frac{c_0V_0}{V}=n_w+\alpha\frac{V_0}{V} \tag{9}$$

where n_w is the refractive index of water (1.3330), α' a proportionality constant, c_0 the 0.2 osmolar sucrose expressed in moles per liter, and $\alpha=\alpha' c_0$. The refractive index of the medium is constant and can be expressed as $n_m=n_w+\beta$. Since $\langle a^4\rangle=(V/V_0)^{4/3}\langle a_0^4\rangle$, Eq. (8) becomes

$$\frac{\mathrm{OD}}{\mathrm{OD}_0}=\left(\frac{V}{V_0}\right)^{4/3}\frac{(\alpha[V_0/V]-\beta)^2}{(\alpha-\beta)^2}. \tag{10}$$

---

2 In this paper, the term *osmolarity* refers to the quantity $\varphi\,\Sigma\nu_i m_i$ where m_i is the molal concentration of the ith solute, the stoichiometric coefficient ν_i is the number of particles produced by dissociation of the ith solute, φ is the molal osmotic coefficient of the solvent, and the summation extends over all the solutes in the solution. The osmolarity is therefore equal to Π/RT where Π is the osmotic pressure, R is the gas constant, and T is the absolute temperature. The terms *hypertonic* and *hypotonic* refer to solutions with osmolarities greater than or less than the osmolarity of the fluid in the vesicle interior.

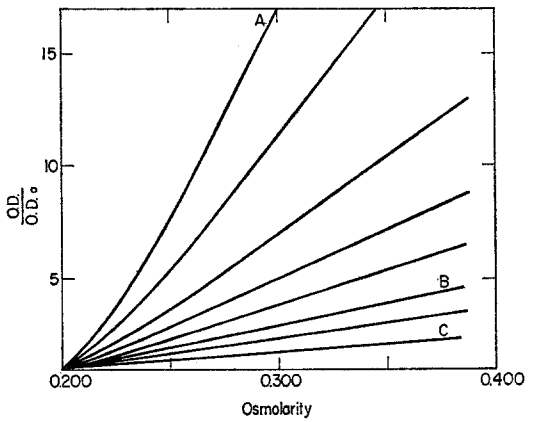

Fig. 4. Calculated OD *vs.* osmolarity of the medium. Eqs. (10) and (11) were used to calculate the relative OD as a function of osmolarity. The initial internal refractive index difference ($n_w + \alpha$) was assumed to be that of 0.2 osmolar sucrose (1.3422). The refractive index of the medium is $n_w + \beta$ where n_w is the refractive index of water (1.3330). A different value of β was assumed for each curve. In the direction *A* to *C*, the values were ($\times 10^{-3}$): 8.3, 8.0, 7.5, 7.0, 6.5, 5.8, 5.0, 3.4. The curves marked *A*, *B* and *C* correspond to the experimental curves *A*, *B* and *C* in Fig. 5. Curve *C* shows a slight curvature near the origin, but this cannot be detected as it is drawn in the figure

The OD ratio thus depends only on the relative volume change of the vesicles and the initial refractive index difference, $\alpha - \beta$.

Eq. (10) was evaluated by assuming that vesicles shrank in hypertonic media until the internal and external osmolarities became equal (Reeves & Dowben, 1969). Thus $c(V-b) = c_0(V_0-b)$, or

$$\frac{V}{V_0} = \frac{c_0}{c}\left(1 - \frac{b}{V_0}\right) + \frac{b}{V_0} \tag{11}$$

where the osmolar concentrations c and c_0 are taken to be equal to the osmolarity of the external medium, and b is the volume of dissolved sucrose in the vesicle interior (b/V_0 calculated from the specific gravity of 0.2 M sucrose is 0.042).

Eqs. (1)–(3), (10) and (11) were used to calculate points for the curves shown in Fig. 4. The family of curves in Fig. 4 depicts the OD changes predicted for immersion of vesicles in various hypertonic media with a particular refractive index.

The theoretical predictions were checked by suspending vesicles prepared in 0.2 M sucrose in various hypertonic media, each with a refractive index of 1.3388. A linear relation between OD and osmolarity of the suspending medium was found (Fig. 5, curve *B*). The refractive indexes of the hypertonic media plotted in curve *A* were all 1.3413 whereas those plotted in curve *C* were all 1.3364; both curves display nonlinearity near the origin. The experimental curves *A*, *B* and *C* in Fig. 5 correspond to the calculated curves *A*, *B* and *C* in Fig. 4. Although the general shapes of the theoretical and experimental curves are similar, the slopes of the linear portions of the theoretical curves are greater than the experimental slopes. The ratios of theoretical to experimental slopes for curves *A*, *B* and *C* are 4.1, 2.0 and 2.1, respectively; the discrepancy may partly be the result of light scattering by the vesicle walls. The observation that a refractive index exists for which OD is a linear function of osmolarity is important when vesicle volume changes are assessed in permeability experiments.

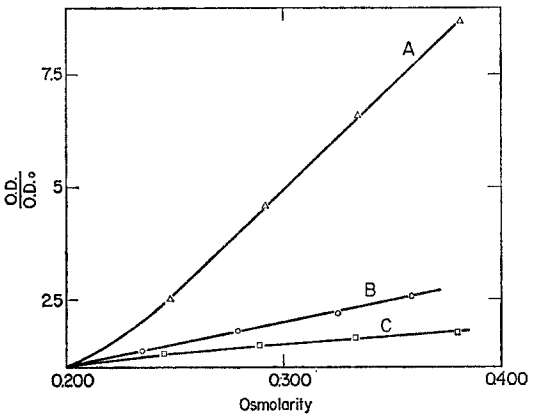

Fig. 5. OD *vs.* the osmolarity of the medium. Curve *A*: Vesicles were prepared in 0.2 M sucrose and suspended in a mixture of 0.2 M glycine and 0.2 M sucrose. The proportions of the glycine and sucrose were adjusted to give a refractive index of 1.3413. Samples of the suspension were mixed with hypertonic solutions of glycine and sucrose, also adjusted to a refractive index of 1.3413. The OD and osmolarity of the suspensions were then determined. Curve *B*: Same as *A*, except that the refractive index of the medium was held constant at 1.3388. Curve *C*: Same as *A*, except that NaCl solutions were used instead of glycine and the refractive index of the medium was held constant at 1.3364. The OD is expressed as a ratio to the OD of the suspension in isotonic media ($\approx$0.2 osmolar). The curves have been shifted slightly so that the initial osmolarity is 0.200 osmolar for each curve

Permeability of Vesicles in Water

When vesicles are placed in a hypertonic glycine media, they shrink; if the refractive index of the external medium is 1.3388, the OD of the suspension is inversely proportional to the vesicle volume after equilibrium is reached. Owing to the fact that vesicles with a range of diameters are present in the suspension, however, the OD change during the period when the vesicles are changing volume is complex. The large vesicles (with a smaller surface/volume ratio) reach equilibrium more slowly than the small vesicles. The relation between OD change and vesicle volume was derived in the following manner.

The vesicle population was divided into discrete classes according to diameter. Within each class, the range of vesicle diameters was sufficiently small that the OD could be regarded to be inversely proportional to vesicle volume. It also was assumed that each class contributed to the total turbidity in proportion to the number of vesicles of that class and to a^4. With these assumptions, the total OD is given by

$$\mathrm{OD} = k \sum \frac{V_0}{V} a_0^4 \, p(a_0) \tag{12}$$

where the summation extends over all classes within the population and for the vesicles within each class; V_0 is the initial volume, V the volume at time t after mixing, a_0 the initial radius, $p(a_0)$ the fraction of vesicles in the class with an arithmetic mean initial radius a_0, and k a proportionality constant.

The rate of change of vesicle volume within each class can be obtained by using the flux equation

$$dV/dt = P_w V_w A \Delta c \tag{13}$$

where A is the surface area of the vesicle, V_w the molar volume of water, V the vesicle volume, Δc the difference of osmolarity across the membrane, and P_w the classical osmotic permeability coefficient. Not all vesicles can be characterized by the same P_w owing to the fact that a fraction of the vesicles are bounded by more than a single bilayer (Reeves & Dowben, 1969). The simplifying assumption is made that all vesicles have the same permeability; the uncertainties of interpretation which this assumption creates are discussed below.

Expressing Δc in terms of vesicle volume (Eq. (11)), and assuming that the vesicles remain spherical during shrinkage, Eq. (13) can be integrated (Lucke, Hartline & McCutcheon, 1931) to yield

$$\frac{P_w t}{a_0} = \frac{a_\infty}{3 c_\infty a_0 V_w}\left[\left(1-\frac{b}{V_\infty}\right)\left\{\frac{1}{2}\ln\frac{1+r^{1/3}+r^{2/3}}{(1-r^{1/3})^2} + \sqrt{3}\arctan\left(\frac{2r^{1/3}+1}{\sqrt{3}}\right)\right\} - 3r^{1/3}\right]_{V_0}^{V} \tag{14}$$

where r is the volume ratio V/V_∞, and a_0 and a_∞ the initial and equilibrium radii of the vesicles. The use of Eq. (14) is simplified greatly by plotting $P_w t/a_0$ against the volume ratio V_0/V.

Plots of calculated OD *vs.* time were constructed using. Eqs. (12) and (14). A value of $P_w t$ was assumed and the ratio V_0/V was obtained from a plot of Eq. (14) for each of 41 vesicle size classes for values of a_0 ranging from 0.4 to 8.4 μ by 0.2 μ increments. The summation of Eq. (12) was performed and the process repeated for other values of $P_w t$. Finally, $P_w t$ was plotted against $(OD - OD_0)/(OD_\infty - OD_0)$, where the subscripts 0 and ∞ refer to the initial and equilibrium conditions, respectively. The water permeability coefficient was determined by comparing this curve with the experimental OD changes and choosing the P_w which gave the best fit.

Effect of Unstirred Water Layers on Measured Permeability Coefficients

When a substance passes through a membrane, concentration gradients are established in the aqueous phases adjacent to the membrane surfaces. As a consequence, the concentration gradient across the membrane itself is reduced, and the permeability coefficient may be underestimated (Dainty, 1963; Vreeman, 1966). The importance of unstirred water layers may be assessed in the following manner.

Although the equation for diffusion from a sphere has not been solved for the boundary conditions pertinent to permeability studies, Vreeman (1966) suggested that the solution for the region external to a sphere with constant surface concentration might provide a rough estimate of the effects of unstirred water layers. We will make the same assumption and solve the equations for the quasi-stationary state, which is attained within a few tenths of a second after mixing.

Assume that the vesicle is a sphere of radius a suspended in an aqueous glycine solution with a constant concentration of glycine at its surface. In the steady state, the amount of water diffusing from a spherical surface of radius r is a constant quantity given by

$$\mathfrak{J}_w = -4\pi r^2 D(\partial c_w/\partial r) \tag{15}$$

where c_w is the concentration of water. For dilute solutions, such as the glycine solutions used in these experiments, the interdiffusion coefficient is approximately equal to the solute diffusion coefficient, $D \approx D_s$.

If there is no volume change on mixing $V_w c_w + V_s c_s = 1$, and

$$V_w(\partial c_w/\partial r) + V_s(\partial c_s/\partial r) = 0 \tag{16}$$

where V_w and V_s are the molar volumes of water and glycine respectively, and c_s is the concentration of solute. Thus, Eq. (15) becomes

$$\mathfrak{J}_w = -4\pi r^2 D \frac{V_s}{V_w} \frac{\partial c_s}{\partial r}. \tag{17}$$

Integrating Eq. (17) for the boundary conditions $c_s = c_\infty$ at $r = \infty$, and $c_s = c_a$ at $r = a$, yields

$$\mathfrak{J}_w = -4\pi a D \frac{V_s}{V_w}(c_a - c_\infty). \tag{18}$$

The true permeability coefficient, P, and an apparent permeability coefficient, P_{app}, are defined by (Vreeman, 1966)

$$\mathfrak{J}_w = -4\pi a^2 P(c_i - c_a) = -4\pi a^2 P_{app}(c_i - c_\infty) \tag{19}$$

where c_i is the solute concentration in the vesicle interior.

Solving Eqs. (18) and (19), one obtains

$$\frac{P_{app}}{P} = \frac{c_i - c_a}{c_i - c_\infty} = \left[1 + \frac{PV_w}{DV_s} a\right]^{-1}. \tag{20}$$

Results

Water Permeability

Calculated and experimental curves for $(OD - OD_0)/(OD_\infty - OD_0)$ *vs.* t at 37 °C are depicted in Fig. 6. A permeability coefficient of 6.8×10^{-3} cm/sec was chosen so that the two curves would coincide at the half time. The experimental curve deviates from the calculated curve at times greater than the half time. The experimental curve showed the same deviations from theory when the osmotic gradient (and hence V_0/V_∞) was reduced to 25% of its value in Fig. 6. The deviation may result in part from the presence of stagnant layers of water at the surfaces of the larger vesicles which lower the apparent permeability of the vesicles, and in part to vesicles with walls of more than one bilayer, a consideration neglected in calculating the theoretical curve. However, membrane thickness in the vesicles does not change as they shrink. Microscopic observations indicate that the excess membrane material in shrunken vesicles is extruded as tiny filaments or spherules which remain attached to the vesicle membrane. Thus, the permeability of the vesicles probably remains constant as they shrink.

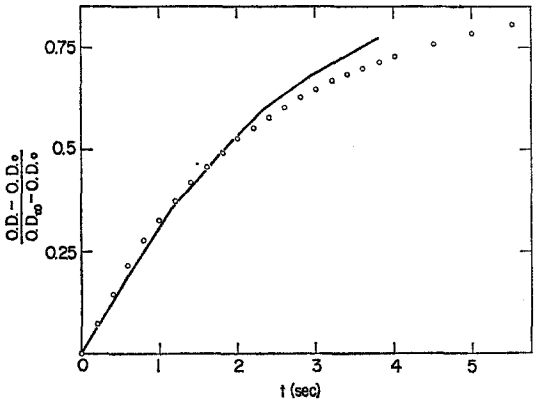

Fig. 6. Experimental and theoretical OD changes during shrinkage of the vesicles. The theoretical curve (solid) was calculated as described in the text. Each point on the experimental curve (circles) represents an average of seven runs. A permeability coefficient of 68.5 μ/sec was chosen so the two curves would coincide at the half time

The water permeability coefficients at 25 and 37 °C for vesicles prepared from three different batches of phospholipids are shown in Table 2. When a single batch of phospholipids was used to prepare the vesicles, the permeability coefficient increased gradually over a period of 3 weeks to about 150% of its original value. The peroxide content of the lipids, monitored by the TBA test, also increased during this time. Thus, small amounts of lipid oxidation appeared to increase the water permeability of the vesicles. The results for preparations A and B (Table 2) were obtained less than 1 week after the lipids were prepared. Preparation C had been stored for 3 months at −30 °C in an evacuated sealed ampoule. Despite these precautions, the peroxide content of the lipids had increased considerably

Table 2. *Permeability coefficient for water*

Lipid prep.	Permeability coefficient (μ/sec)[a]	
	25 °C	37 °C
A	40.6	–
B	44.8	68.5
C	48.9	90.6

[a] Permeability coefficients were calculated from the half time of the OD change, as illustrated in Fig. 6. The half times were the average of five to seven different runs. The average standard error for these determinations was 3%; the temperatures given here were ±2°.

during this period. The results in Table 2 for preparation C were obtained immediately after the ampoule was opened.[3]

Temperature Dependence of Water Permeability

The water permeability coefficient of the vesicles is plotted against the reciprocal of the absolute temperature in Fig. 7 for two different lipid preparations. Assuming that the permeability coefficient has the form

$$P = P_0 \exp[-\Delta E_P / RT] \tag{21}$$

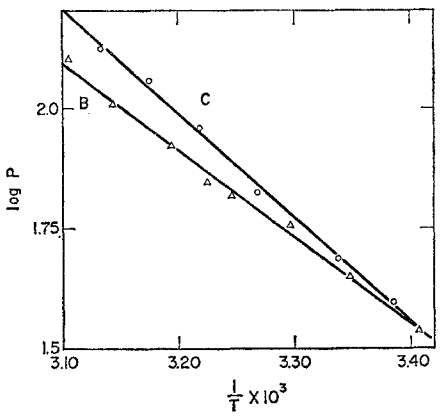

Fig. 7. Permeability coefficient *vs.* the reciprocal of the absolute temperature. At each temperature, the permeability coefficient was determined from the average half time of five to seven runs. Curves for vesicles prepared from two different lipid preparations are shown

3 Sha'afi *et al.* (1967) studied the volume changes in human erythrocytes by light scattering in a stopped flow apparatus after mixing with a hyperosmolar solution. The half time of volume change in Fig. 8 of Sha'afi *et al.* (1967) is 0.20 sec compared to 1.85 sec in Fig. 6 of our studies. Yet Sha'afi *et al.* calculated $P_w = 122$ μ/sec whereas we report $P_w = 68$ μ/sec. The apparent discrepancy between their results and ours arises because the two sets of data cannot be compared directly, because erythrocytes, unlike phospholipid vesicles, are homogeneous in size, nonspherical, and because the half time of OD changes in turbidity experiments is not identical to the half time of volume changes. The results of Sha'afi *et al.* (1967) and ours can be compared in the following manner.

The rate of entry of water into erythrocytes is related to the surface/volume ratio, not the largest cellular diameter. Using the data of Sha'afi *et al.* ($V = 87 \times 10^{-12}$ cm^3/cell, and $A = 1.67 \times 10^{-6}$ cm^2/cell), the surface/volume ratio of a human erythrocyte is equal to that of a sphere of radius 1.57 μ. Assuming $P_w = 122$ μ/sec and $b/V_0 = 0.428$ (Savitz *et al.*, 1964), the half time of volume change for a sphere this size using the conditions of Sha'afi *et al.* ($c_\infty/c_0 = 1.49$) is calculated to be 0.216 sec from Eq. (14). This compares closely to the value of 0.20 sec obtained directly from the data of Sha'afi *et al.* It should be noted that Eq. (14) takes into account the reduction in surface area upon shrinkage (necessary for phospholipid vesicles), whereas Sha'afi *et al.* assumed that the surface area remains constant (probably correct for erythrocytes).

Table 3. *Activation energy for water transport*

Lipid prep.	E_p (kcal/mole)	P_0 (cm/sec)
B	8.25 ± 0.25	4.84×10^3
C	9.85 ± 0.31	7.49×10^4

where ΔE_P is the activation energy, and P_0 a constant; the slope of such a curve can be used to obtain the activation energy for water permeation.

Values for P_0 and ΔE_P are summarized in Table 3. The higher activation energy obtained for preparation C does not reflect the partially oxidized condition of the lipids; an even more highly oxidized preparation yielded an activation energy of 7.5 ± 0.3 kcal/mole. Tien and Ting (1968) obtained an activation energy of 6.8 kcal/mole for water transport across bilayer membranes of oxidized cholesterol. Redwood and Haydon (1969) found an activation energy of 14.6 kcal/mole for water transport across lecithin-cholesterol-hydrocarbon bilayer membranes; Price and Thompson (1969) reported values of 12.7 and 13.1 kcal/mole for similar membranes. For water transport across cellular membranes, activation energies between 2.5 and 17 kcal/mole have been reported (Dick, 1966).

Discussion

Although permeability measurements generally have been fraught with many kinds of imprecision, mention should be made of some particular kinds of uncertainties encountered in these studies which arise from the experimental conditions employed as well as from simplifying assumptions made in the analysis.

Some of the light seen by the photomultiplier tube in the spectrophotometer is due to low angle scatter. Because the analysis was semi-empirical and did not require measurement of absolute extinction coefficients, the effect was not considered. This may lead to some distortion of the results, however, because the fraction of light scattered at low angles increases with the size of the vesicles (Billmeyer, 1964). Neglecting low angle scattering therefore results in an overestimate of the contribution of the larger vesicles to the total turbidity and, in turn, in an overestimate of the permeability coefficient.

Some idea of the magnitude of this error can be obtained by assuming the extreme position that all vesicles have the geometric mean radius 0.87μ. With this assumption, a permeability coefficient of 21.6 μ/sec is obtained from the data in Fig. 6, compared to the value of 68.5 μ obtained by the

Table 4. *P_{app}/P of water as a function of vesicle radius*

Radius (μ)	1	3	5	7
P_{app}/P [a]	0.976	0.932	0.891	0.854

[a] P_{app}/P was calculated using Eq. (20) for several different radii, assuming $P = 7 \times 10^{-3}$ cm/sec, $D = 1.1 \times 10^{-5}$ cm^2/sec, $V_w = 18$ cm^3 and $V_s = 47$ cm^3; V_s was taken to be equal to the apparent molar volume of glycine.

method discussed in the paper. The former value represents a minimum estimate of P_w because it does not take into account the relatively greater contribution of the larger vesicles.

In the above analysis, it was assumed that the vesicles are all bounded by a single bilayer. However, phospholipid analyses of vesicle suspensions suggest that some vesicles are bounded by more than one bilayer. Thus, the permeability coefficients calculated in these experiments may have underestimated the permeability of a single bilayer by a factor of two or three.

Another source of uncertainty is the presence of stagnant layers of water at the surface of the vesicle membranes. The ratio $P_{app}/P_w = 7 \times 10^{-3}$ cm/sec is listed in Table 4 for spheres of various radii. Unstirred water layers may cause an underestimate of the permeability coefficient, but the effect is likely to be small. Using a different approach, Sha'afi, Rich, Sidel, Bossert and Solomon (1967) found only a minor effect on the water permeability of erythrocytes attributable to bulk phase diffusion. Because the ratio P_{app}/P decreases with increasing radius, the effective permeability of large vesicles may be less than that of small vesicles. These factors, which were not considered in evaluating OD changes in our experiments, may explain part of the differences between the experimental data and theoretical predictions (Fig. 6). In fact, experiments in this laboratory show the deviations between experimental and theoretical values were less when the volume changes were produced by isosmotic penetration of slightly permeable solutes such as glycerol or urea. In the latter experiments, water flow was so slow that bulk phase diffusion could not have had a measurable effect upon the results.

Because the above errors partially offset one another, it is difficult to estimate the accuracy of the reported permeability coefficients. The permeability coefficients found in these studies are similar to those reported for phospholipid bilayer membranes formed across an aperture in a thin plastic diaphragm (Huang & Thompson, 1966; Hanai, Haydon & Redwood, 1966; Cass & Finkelstein, 1967), and fall within the range of osmotic permeabilities reported for biological membranes, 0.4 to 200 μ/sec (Dick, 1966).

It has been suggested that water molecules cross lipid membranes by diffusing through aqueous channels (Huang & Thompson, 1966), by dissolving and diffusing within the hydrocarbon interior of the membrane (Hanai & Haydon, 1966; Vreeman, 1966; Redwood & Haydon, 1969; Price & Thompson, 1969), or by traversing, in a single jump, a highly ordered array of water molecules at the membrane-water interfaces (Tien & Ting, 1968). Aqueous pores are thought to be absent from bilayer membranes formed across an aperture owing to the high electrical resistance of these membranes and the equivalence of osmotic and isotopic permeability coefficients for water (Cass & Finkelstein, 1967; Tien & Ting, 1968). Similar evidence has not yet been obtained for phospholipid vesicles, but the low permeability to glycine suggests that pores are not present in sufficient numbers to account for the high permeability of vesicles for water. The single-jump mechanism proposed by Tien and Ting (1968) cannot be excluded although it must be said that the evidence advanced to support this theory is not very convincing. The dissolution-diffusion mechanism is favored by several investigators, probably because it is conceptually attractive, consistent with the data (*see* below) and amenable to quantitative analysis. It should be pointed out, however, that permeability measurements alone do not provide enough information to suggest a choice between any of these alternatives.

An analysis of the solubility-diffusion mechanism in terms of absolute reaction rate theory will serve to illustrate some of its important features. If diffusion through the hydrocarbon interior of the membrane is the rate-limiting process in water permeation, the permeability coefficient can be expressed as

$$P_w = V_w X_w D_w / V_h \Delta x \tag{22}$$

where V_w and V_h are the molar volumes of water and hydrocarbon, respectively, X_w the mole fraction of water in the hydrocarbon, D_w the diffusion coefficient of water within the membrane, and Δx the thickness of the hydrocarbon layer.

According to absolute reaction rate theory (Glasstone, Laidler & Eyring, 1941), the diffusion coefficient is given by

$$D = e \frac{\lambda^2 \kappa T}{h} \exp\left[\frac{\Delta S^{\ddagger}}{R}\right] \exp\left[-\frac{\Delta E_D}{RT}\right] \tag{23}$$

where $\Delta S^{\ddagger}$ is the entropy of activation, ΔE_D the experimental activation energy, λ the distance between successive equilibrium positions along the path of diffusion, κ Boltzmann's constant, and h Planck's constant. The

solubility X_w is an equilibrium constant and

$$RT\ln X_w = T\Delta S^0 - \Delta H^0 = -\Delta G^0 \tag{24}$$

where ΔH^0 and ΔS^0 are the standard heat and standard entropy of solution.

The permeability coefficient can be expressed by a relation in the form of Eq. (21) with $\Delta E_P = \Delta H^0 + \Delta E_D$; thus,

$$P_0 = e\frac{\lambda^2 \kappa T}{\eta \Delta x}\frac{V_w}{V_h}\exp\left[\frac{\Delta S^0 + \Delta S^{\neq}}{R}\right]. \tag{25}$$

Assuming a single lipid bilayer corresponds to a layer of lipid hexadecane 50-A thick, the values P_w, $(\Delta H^0 + \Delta E_D)$, and $(\Delta S^0 + \Delta S^{\neq})$ can be calculated from Eq. (25) (*see* Table 5). Two sets of values are given based on the solubility data for water in hexadecane as determined by Schatzberg (1963) and by Englin, Plate, Tugolukov and Pryanishnikov (1965). In these calculations, values used were $D_w = 4.16$ cm^2/sec (25 °C), $\Delta E_D = 3.4$ kcal/mole and $\Delta S^{\neq} = 2.2$ e.u. (Schatzberg, 1965); and $\lambda = 1.5$ A was assumed, a value often found for diffusion in nonpolar solvents (Glasstone *et al.*, 1941). Considering the assumptions and approximations, the agreement between the two sets of data is good. Clearly, the contributions of the heat and entropy of solution cannot be neglected in assessing the experimental quantities ΔE_P and P_0 as they sometimes have in the past (Zwolinski, Eyring & Reese, 1949; Davson & Danielli, 1952; Scheuplein, 1968).

The diffusion and solubility properties of the lipid membrane are undoubtedly more complex than hexadecane. The hydrocarbon chains in the lipid bilayer are more ordered than those in liquid hexadecane, probably lowering the diffusion coefficient of water in the membrane. Cholesterol markedly

Table 5. *Theoretical permeability properties*[a]

Data of	P_w (μ/sec)		$\Delta E_p = \Delta H^0 + \Delta E_D$	$S^0 + S^{\neq}$ (e.u.)
	25 °C	37 °C	(kcal/mole)	
Englin *et al.* (1965)	59.9	140.9	13.35	22.1
Schatzberg (1965)	34.7	70.5	11.5	15.0
This paper				
prep. B	44.8	68.5	8.25	4.6
prep. C	48.9	90.6	9.85	10.1

[a] The quantities given were calculated from Eqs. (22) and (25) using the solubility data given in Table 6. The experimental results are included for comparison. The experimental value for $\Delta S^0 + S^{\neq}$ was obtained from Eq. (25), with $\Delta x = 50$ A, $\lambda = 1.5$ A, $T = 300$ °K and $V_h = 293$ cm^3 (the molar volume of hexadecane).

reduces the mobility of phospholipid hydrocarbon chains, certainly in liquid crystals of egg lecithin (Chapman & Penkett, 1966). An interaction of this kind is expected to lower the diffusion coefficient and increase the activation energy for water permeation. The higher activation energies for water permeability reported by Redwood and Haydon (1969) and Price and Thompson (1969) may be due to the use of membranes which contained unknown but probably significant amounts of cholesterol. Finkelstein and Cass (1967) reported that bilayer membranes formed across a diaphragm aperture from cholesterol-containing phospholipid solutions had lower water permeability than cholesterol-free bilayer membranes. Preliminary experiments performed with cholesterol-containing vesicles in our laboratory also show lower water permeability than for cholesterol-free vesicles.

The hydrocarbon chains of the phospholipids vary in length and degree of unsaturation. Hildebrand and Scott (1964), noticing the greater solubility of water in olefins than in the analogous alkanes, suggested that the water molecules approach and polarize the double bond of the olefin. Specific interactions of this type might lead to a decrease in both the heat and entropy of solution, thus bringing the theoretical predictions closer to the experimental data.

Table 6 gives the solubility of water in various hydrocarbons at 20 °C together with the standard heats and entropies of solution calculated from the data of Schatzberg (1963) and Englin *et al.* (1965). The heats and entropies of solution show little variation with the length of the hydrocarbon molecules, but are influenced profoundly by the degree of unsaturation. The large values of ΔH^0 and ΔS^0 for saturated hydrocarbons reflect the fact that water molecules are passing from the propagated hydrogen-bonded

Table 6. *Solubility of water in various hydrocarbons*[a]

Hydrocarbon	$X_w(\times 10^4)$	ΔH^0 (kcal/mole)	ΔS^0 (e.u.)
Heptane[b]	5.3	10.4	20.4
Heptene[b]	13.6	5.9	7.1
Octane[b]	6.0	10.0	19.4
Octene[b]	22.1	4.8	4.1
Hexadecane[b]	8.7	9.95	19.9
Hexadecane[c]	5.5	8.1	12.8

[a] The standard state of water in the aqueous phase was assumed to be the pure liquid at 20 °C. For the hydrocarbon phase, the standard state for water was an activity of one at the experimental temperature. The activities were assumed to be equal to the mole fraction at low concentrations.

[b] Calculated from the data of Englin *et al.* (1965).

[c] Calculated from the data of Schatzberg (1965).

structure of the aqueous phase into the hydrocarbon phase where the interaction between neighboring molecules is comparatively small. The lower ΔH^0 and ΔS^0 for unsaturated hydrocarbons may reflect specific water-olefin interactions of the type described by Hildebrand and Scott (1964). In contrast to these results, Finkelstein and Cass (1967) found that the water solubility in 1-hexadecene was only 15% greater than in hexadecane. However, the water permeability of a bilayer membrane prepared from hydrogenated egg lecithin was less than half that of a natural lecithin bilayer.

Although the data derived from the present studies are consistent with a dissolution-diffusion mechanism, further studies are needed to establish its validity. It also is clear that the success of the model in describing permeability characteristics of lipid bilayers does not imply that the structural properties of membranes and bulk hydrocarbon are identical.

The authors wish to thank Dr. Thayer C. French for the use of his stopped flow apparatus. This research was supported in part by grant GB-5474 from the National Science Foundation. Dr. Reeves was supported by a Predoctoral Fellowship from the National Institute of General Medical Sciences.

References

Ansell, G. B., Hawthorne, J. N. 1964. Phospholipids: Chemistry, Metabolism and Function. Elsevier, Amsterdam.

Bangham, A. D., Standish, M. M., Watkins, J. C. 1965. Diffusion of univalent ions across the lamellae of swollen phospholipids. *J. Mol. Biol.* **13**:238.

Billmeyer, F. W., Jr. 1964. Principles of light scattering. *In:* Treatise on Analytical Chemistry, part I, vol. 5. I. M. Kolthoff, P. J. Elving and E. B. Sandell, editors. p. 2839. Interscience, New York.

Blank, M., LaMer, V. I. 1962. The energy barrier for monolayer penetration. *In:* Retardation of Evaporation by Monolayers: Transport Processes. V. K. LaMer, editor. p. 59. Academic Press, New York.

Cass, A., Finkelstein, A. 1967. Water permeability of thin lipid membranes. *J. Gen. Physiol.* **50**:1765.

Chapman, D., Penkett, S. A. 1966. Nuclear magnetic resonance spectroscopic studies of the interaction of phospholipids with cholesterol. *Nature* **211**:1304.

Dainty, J. 1963. Water relations of plant cells. *Advanc. Bot. Res.* **1**:279.

Davson, H., Danielli, J. F. 1952. The Permeability of Natural Membranes. Cambridge University Press, Cambridge.

Dick, D. A. T. 1966. Cell Water. Butterworths, Washington.

Englin, B. A., Plate, A. F., Tugolukov, V. M., Pryanishnikov, M. A. 1965. *Khim. Tekhnol. Topliv Masel* **10**:42.

Finkelstein, A., Cass, A. 1967. Effect of cholesterol on the water permeability of thin lipid membranes. *Nature* **216**:717.

French, T. C., Benkovic, S. J., Bruice, T. C. 1965. Stopped flow apparatus for a Zeiss PMQ-11 spectrophotometer. *Rev. Sci. Instr.* **36**:860.

Glasstone, S., Laidler, K. J., Eyring, H. 1941. The Theory of Rate Processes. McGraw-Hill, New York.

Hanai, T., Haydon, D. A. 1966. The permeability to water of bimolecular lipid membranes. *J. Theoret. Biol.* **11**:370.

— — Reswood, W. R. 1966. The water permeability of artificial bimolecular leaflets: A comparison of radiotracer and osmotic methods. *Ann. N.Y. Acad. Sci.* **137**:731.

Hildebrand, J. H., Scott, R. L. 1964. The Solubility of Nonelectrolytes. Dover, New York.

Hochgesang, F. P. 1964. *In:* Treatise on Analytical Chemistry, part I, vol. 5. I. M. Kolthoff, P. J. Elving and E. B. Sandell, editors. p. 3289. Interscience, New York.

Huang, C., Thompson, T. E. 1966. Properties of lipid bilayer membranes separating two aqueous phases: Water permeability. *J. Mol. Biol.* **15**:539.

— Wheeldon, L., Thompson, T. E. 1964. The properties of lipid bilayer membranes separating two aqueous phases: Formation of a membrane of simple composition. *J. Mol. Biol.* **8**:148.

Koch, A. L. 1961. Some calculations on the turbidity of mitochondria and bacteria. *Biochim. Biophys. Acta* **51**:429.

Lucke, B., Hartline, H. K., McCutcheon, M. 1931. Further studies on the kinetics of osmosis in living cells. *J. Gen. Physiol.* **14**:405.

Mueller, P., Rudin, D. O., Tien, H. T., Wescott, W. C. 1963. Methods for the formation of single bimolecular lipid membranes in aqueous solution. *J. Phys. Chem.* **67**:534.

Ottolenghi, A. 1959. Interaction of ascorbic acid and mitochondrial lipides. *Arch. Biochem. Biophys.* **79**:355.

Price, H. D., Thompson, T. E. 1969. Properties of liquid bilayer membranes separating two aqueous phases: Temperature dependence of water permeability. *J. Mol. Biol.* **41**:443.

Redwood, W. R., Haydon, D. A. 1969. Influence of temperature and membrane composition on the water permeability of lipid bilayers. *J. Theoret. Biol.* **22**:1.

Reeves, J. P., Dowben, R. M. 1969. Preparation and properties of thin-walled phospholipid vesicles. *J. Cell. Physiol.* **73**:49.

Rendi, R. 1964. Water extrusion in isolated subcellular fractions. *Biochim. Biophys. Acta* **84**:694.

Savitz, D., Sidel, V. W., Solomon, A. K. 1964. Osmotic properties of human red cells. *J. Gen. Physiol.* **48**:70.

Schatzberg, P. 1963. Solubilities of water in several normal alkanes from C_7 to C_{16}. *J. Phys. Chem.* **67**:776.

— 1965. Diffusion of water through hydrocarbon liquids. *J. Polymer Sci. C* **10**:87.

Scheuplein, R. J. 1968. On the application of rate theory to complex multibarrier flow co-ordinates: Membrane permeability. *J. Theoret. Biol.* **18**:72.

Sha'afi, R. I., Rich, G. T., Sidel, V. W., Bossert, W., Solomon, A. K. 1967. The effect of the unstirred layer on human red cell water permeability. *J. Gen. Physiol.* **50**:1377.

Tien, H. T., Ting, H. P. 1968. Permeation of water through bilayer lipid membranes. *J. Colloid Interface Sci.* **27**:702.

van de Hulst, H. C. 1957. Light Scattering by Small Particles. Wiley, New York.

Vreeman, H. J. 1966. Permeability of thin phospholipid films II. *Kon. Ned. Akad. Wetensch. Proc. B* **69**:555.

Zwolinski, B. J., Eyring, H., Reese, C. E. 1949. Diffusion and membrane permeability. *J. Phys. Chem.* **53**:1426.